JACS
JOURNAL OF THE AMERICAN CHEMICAL SOCIETY
COMMUNICATION
pubs.acs.org/JACS

# A Rapid Electrochemical Method for Determining Rate Coefficients for Copper-Catalyzed Polymerizations

Craig A. Bell,[†] Paul V. Bernhardt,[*,‡] and Michael J. Monteiro[*,†]

[†]Australian Institute for Bioengineering and Nanotechnology and [‡]School of Chemistry and Molecular Biosciences, University of Queensland, Brisbane 4072, Australia

S *Supporting Information*

**ABSTRACT:** Copper(I) polyamine complexes have emerged as excellent atom-transfer radical polymerization catalysts. The rate of their reaction with organic halide initiators (the so-called activation step) varies across a broad range, depending on both the structure of the copper complex and the initiator. Herein, we report a new technique for determining the rate of copper-catalyzed activation ($k_{act}$) using cyclic voltammetry coupled with electrochemical simulation. This method is applied to measuring $k_{act}$ for one of the most active catalysts, $[Cu^I(Me_6tren)]^+$ ($Me_6tren$ = *N,N,N*-tris-(2-(dimethylamino)ethyl)amine), in reaction with ethyl bromoisobutyrate.

Copper-catalyzed polymerization is a well-established procedure for controlling the molecular weight and molecular weight distribution of a wide range of polymers.[1,2] Obtaining well-defined polymers by atom-transfer radical polymerization (ATRP) is determined by the ratio of rate coefficients for activation of RX (an alkyl halide) and deactivation of $R^\bullet$ by copper complexes ($K_{ATRP}$ in eq 1).

$$Cu^IL + RX \underset{k_{deact}}{\overset{k_{act}}{\rightleftharpoons}} Cu^{II}LX + R^\bullet \quad K_{ATRP} = k_{act}/k_{deact} \quad (1)$$

The effectiveness of the $Cu^I$ complex is very dependent on the nature of the ligand and solvent. Highly active complexes can significantly reduce the amount of copper species to ppm levels in the polymerizations, making such catalysts attractive for industrial-scale polymerizations.[3−13] Although there are methods to determine the activation rate coefficient ($k_{act}$), they are limited to catalysts that have $k_{act} < 2\ M^{-1}\ s^{-1}$. For more active catalysts, stopped-flow spectrophotometric methods are required to measure the formation of $Cu^{II}$ over time,[14] but even this has its limitations in terms of the maximum measurable rate of the bimolecular $Cu^I$/initiator reaction, the inherent air sensitivity, and potential instability toward disproportionation of $Cu^I$-based catalysts.

Herein, we describe a new, robust and straightforward electrochemical method that enables $k_{act}$ to be determined using cyclic voltammetry (CV) and is model-independent in terms of the mechanism of the polymerization reaction that follows. It is not limited by conventional problems associated with direct rapid kinetic measurements using stopped-flow techniques (instrumental and mixing dead times, interference from oxygen), as the reactive $Cu^I$ complexes are generated transiently under strict anaerobic conditions near the electrode surface. The time scale of the experiment separates $k_{act}$ from any other following chemical steps relevant to the polymerization reaction.

We have investigated the highly active copper catalyst $[Cu^I(Me_6tren)]^+$ ($Me_6tren$ = *N,N,N*-tris(2-(dimethylamino)ethyl)amine) in its reaction with the initiator ethyl bromoisobutyrate (EBriB, EtOC(O)CBrMe$_2$, Scheme 1) using CV. X-ray crystal structures of several complexes from the $[Cu^{II}(Me_6tren)(X)]^{n+}$ (X = halide or solvent) family[15,16] in addition to EPR spectroscopy[17−20] and theoretical studies[21,22] have shown that the $Cu^{II}$ complexes are invariably trigonal bipyramidal and the monodentate co-ligand occupies the axial coordination site *trans* to the central tertiary amine. However, the monovalent complex $[Cu^I(Me_6tren)](ClO_4)$ is pseudo-four-coordinate in the solid state, bearing a trigonal pyramidal geometry with the $ClO_4^-$ anion only weakly associated, as shown by X-ray crystallography.[23] Solution equilibrium studies of ternary complexes of $Cu^{II}$ or $Cu^I$ with $Me_6tren$ and bromide have been reported[24] as well as EXAFS solution structural studies,[25] which revealed that several combinations of Cu, amine, and bromide are possible, depending on their relative concentrations.

Cyclic voltammetry of $[Cu^{II}(Me_6tren)]^{2+}$ in the presence and in the absence of bromide in both MeCN and DMSO (Supporting Information (SI) Figure S1) led to separate and reversible $Cu^{II/I}$ couples from both $[Cu^{II}(Me_6tren)(S)]^{2+/+}$ (S = MeCN or DMSO, higher potential) and $[Cu^{II}(Me_6tren)Br]^{+/0}$ (lower potential). The reversibility of the $[Cu(Me_6tren)Br]^{+/0}$ couple indicates that the bromido ligand dissociates only slowly from the $Cu^I$ complex and that $[Cu^I(Me_6tren)Br]$ has an appreciable formation constant. The difference between the $Cu^{II/I}$ redox potentials (volts) with ($E_{Br}$) and without ($E_S$) bromide affords the ratio of the $Cu^{II}$ and $Cu^I$ formation constants ($K_{Cu(II)Br}/K_{Cu(I)Br}$, eq 2),[26] and this has been examined in a number of Cu complexes relevant to ATRP.[27]

$$\log(K_{Cu(II)Br}/K_{Cu(I)Br}) = 16.9(E_S - E_{Br}) \quad at\ 298\ K \quad (2)$$

The $[Cu^{II}(Me_6tren)]^{2+}$:$Br^-$ association constants in DMSO and MeCN (Scheme 1, D; $K_{Cu(II)Br} = k_{IIaBr}/k_{IId,Br}$) were examined independently under the same conditions by spectrophotometric titration (SI Figure S2), and the data were modeled by global analysis with SPECFIT.[28] In MeCN, the complexation reaction was complete after addition of 1 equiv of bromide, yielding a lower bound of $\log K_{Cu(II)Br} \geq 5$. In DMSO, a more gradual saturation of the complex upon bromide addition was seen, and a lower value of $\log K_{Cu(II)Br} = 3.9(3)$ was obtained.

**Received:** June 6, 2011
**Published:** July 11, 2011

**Scheme 1. Catalytic Mechanism for Initiator Activation**

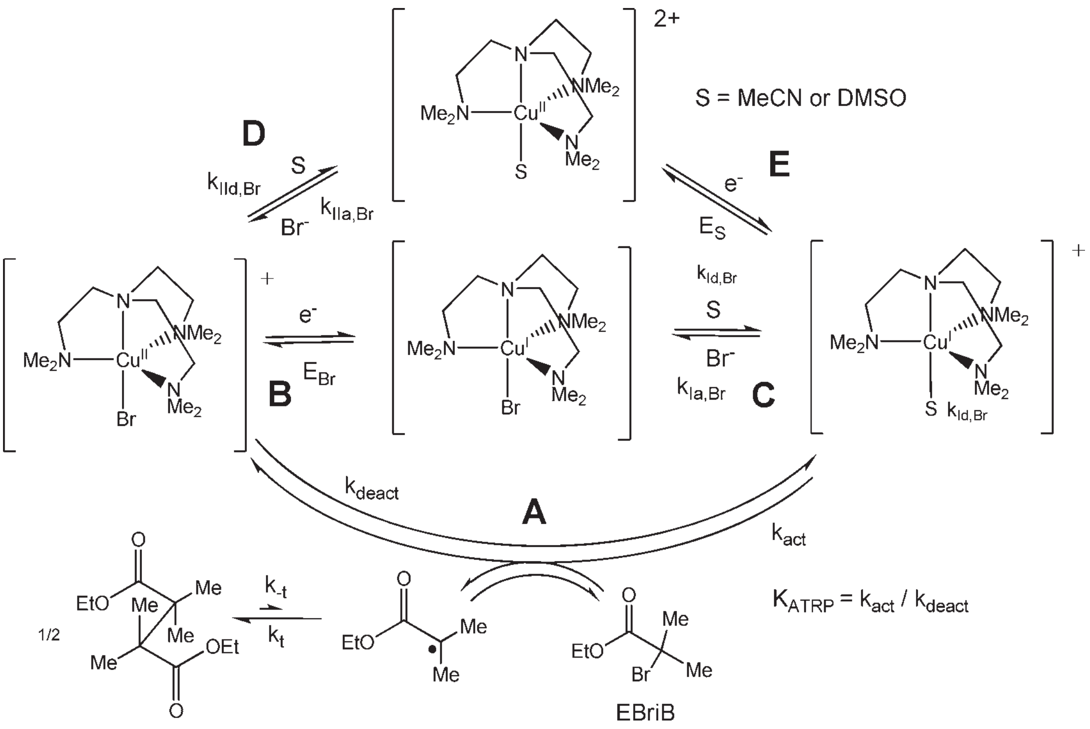

---

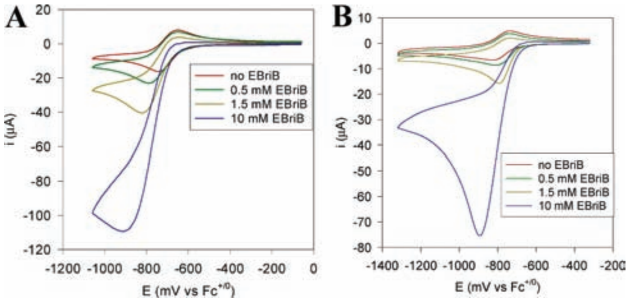

**Figure 1.** Cyclic voltammograms of $[Cu(Me_6tren)Br]Br$ (1 mM) at four different concentrations of EBriB in (A) MeCN and (B) DMSO. All other conditions are the same (50 mV $s^{-1}$ sweep rate, 0.1 M $Et_4NClO_4$, 298 K). All voltammograms were swept initially in the negative direction.

These results are comparable with other published studies,[24] the differences being attibuted to the supporting electrolyte (0.1 M $Et_4NClO_4$) used here to match the electrochemistry experiments. Importantly, at millimolar concentrations of $[Cu^{II}(Me_6tren)Br]Br$, no significant dissociation of $Br^-$ occurs in either MeCN or DMSO, and combined with the electrochemical measurements, the related $Cu^I{-}Br$ formation constants (from eq 2) are also significant ($\log K_{Cu(I)Br} \geq 1.3$ in MeCN and $\log K_{Cu(I)Br} = 2.4$ in DMSO).

Following the activation step, where the Br atom is transferred from EBriB to Cu (Scheme 1, A), the Cu−Br bond must be broken, and reduction to the active $Cu^I$ complex must occur before another molecule of EBriB can react. These two steps *en route* to $[Cu^I(Me_6tren)]^+$, the active copper catalyst,[29] may occur in either order, as shown in Scheme 1 (B→C or D→E), but in any case the bromido ligand association and dissociation rate constants for both oxidation states ($k_{II,a}/k_{II,d} = K_{Cu(II)Br}$ and $k_{I,a}/k_{I,d} = K_{Cu(I)Br}$) are part of the overall catalytic cycle. It is known[30] that the steric effects of the *N*-methyl groups on $Me_6tren$ ligand decrease the rates of ligand exchange on $Cu^{II}$ by ca. 5 orders of magnitude relative to tren. This is evidently one of the key factors in $[Cu^I(Me_6tren)]^+$ being such an effective catalyst.

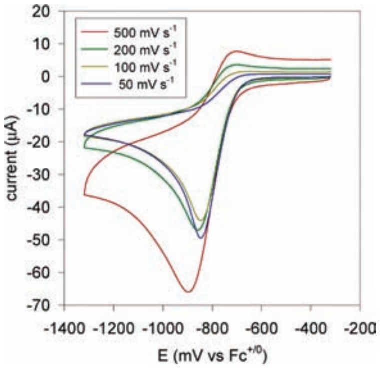

**Figure 2.** Cyclic voltammograms of $[Cu(Me_6tren)Br]Br$ (1 mM) and EBriB (5 mM) in DMSO at four different sweep rates (50, 100, 200, and 500 mV $s^{-1}$). All voltammograms were swept initially in the negative direction at 298 K.

The $Cu^I$-catalyzed activation reaction (Scheme 1, A) was investigated by CV in the presence of EBriB. As mentioned above, $[Cu^{II}(Me_6tren)Br]^+$ is the dominant species in both DMSO and MeCN when $[Cu^{II}(Me_6tren)Br]Br$ is employed as the precursor (see SI). Reduction to $[Cu^I(Me_6tren)Br]/[Cu^I(Me_6tren)(S)]^+$ is coupled to the reversible activation step that regenerates $[Cu^{II}(Me_6tren)Br]^+$, formally a so-called $EC_{cat}$ mechanism (an electron transfer followed by a catalytic chemical reaction).[31]

As expected for an $EC_{cat}$ mechanism, (i) the ratio of anodic and cathodic peak currents ($i_{pa}/i_{pc}$) was less than unity in the presence of

Table 1. Important Rate and Thermodynamic Constants at 298 K for the $[Cu^{II}(Me_6tren)Br]^+$/EBriB System[a]

| | MeCN | DMSO | | MeCN | DMSO |
|---|---|---|---|---|---|
| $k_{deact}$ ($M^{-1}$ $s^{-1}$) | $1.1 \times 10^7$ | $1.1 \times 10^7$ | $k_{I,d,Br}$ ($s^{-1}$) | $7.6 \times 10^1$ | $2.0 \times 10^2$ |
| $k_{act}$ ($M^{-1}$ $s^{-1}$) | $3.7 \times 10^4$ | $8.7 \times 10^4$ | $k_{I,a,Br}$ ($M^{-1}$ $s^{-1}$) | $3.5 \times 10^4$ | $7.7 \times 10^4$ |
| $k_{II,d,Br}$ ($s^{-1}$) | $4.7 \times 10^{-5}$ | $2.0 \times 10^1$ | $E_S$ (mV vs $Fc^{+/0}$) | −500 | −700 |
| $k_{II,a,Br}$ ($M^{-1}$ $s^{-1}$) | $1.3 \times 10^2$ | $1.6 \times 10^5$ | $E_{Br}$ (mV vs $Fc^{+/0}$) | −722 | −787 |

[a] Estimated uncertainties in rate constants are 10%.

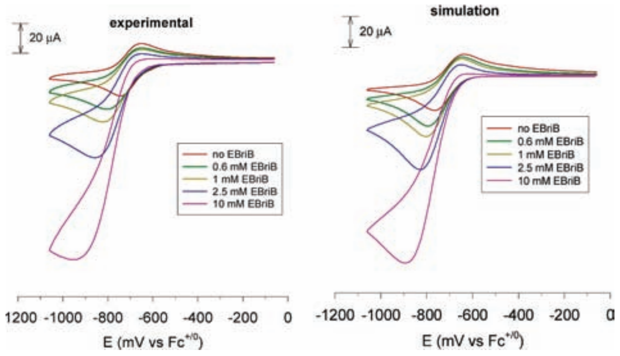

**Figure 3.** Comparison of experimental and simulated cyclic voltammograms of $[Cu(Me_6tren)Br]Br$ (1 mM) at increasing concentrations of EBriB. Sweep rate, 100 mV $s^{-1}$; solvent, MeCN; supporting electrolyte, 0.1 M $Et_4NClO_4$; 298 K.

EBriB, (ii) $i_{pa}/i_{pc}$ was dependent on both sweep rate and EBriB concentration, and (iii) the cathodic current increased with the concentration of EBriB. Typical CV data are illustrated in Figure 1 at different concentrations of EBriB in MeCN and DMSO. The change from a reversible $Cu^{II/I}$ wave in the absence of EBriB to an asymmetric irreversible wave at higher concentrations of EBriB (0.5, 1.5, and 10 mM) is evident. Also, the cathodic current increases markedly with EBriB concentration, confirming the catalytic nature of the process; i.e., $Cu^{II}$ is being chemically regenerated during the cathodic sweep, resulting in an amplification of current.

Increasing the sweep rate partially restores the reversibility of the CV wave ($i_{pa}/i_{pc}$ increases) due to the $Cu^I$ form being reoxidized electrochemically faster than it is consumed in the bimolecular $[Cu(Me_6tren)]^+$/EBriB reaction. This is illustrated for the system in DMSO with 5 mM EBriB present (Figure 2), where at a sweep rate of 50 mV $s^{-1}$ there is no anodic peak ($i_{pa}/i_{pc} = 0$), while at 500 mV $s^{-1}$ the $i_{pa}/i_{pc}$ ratio is restored to 0.28.

Given the complexity of Scheme 1, extraction of meaningful kinetic data can be accomplished only by simulation of the experimental voltammetry. The program DigiSim[32] was employed, and the entire set of simulation parameters (redox potentials, diffusion coefficients, homogeneous and heterogeneous rate coefficients) was obtained. As with any multi-parametrized system, there is a danger of false minima or correlated variables if too many parameters are allowed to vary simultaneously. The heterogeneous rate constant $k_0$, $Cu^{II/I}$ redox potential, and diffusion coefficients ($3 \times 10^{-5}$ $cm^2$ $s^{-1}$ in MeCN or $5 \times 10^{-6}$ $cm^2$ $s^{-1}$ in DMSO) were all obtained by simulating the CV data in the absence of EBriB and held constant thereafter. The deactivation rate coefficient ($k_{deact} = 1.1 \times 10^7$ $M^{-1}$ $s^{-1}$) is well established from other studies[33−35] and was assumed constant in all simulations. Similarly, the radical termination step ($k_t = 1 \times 10^9$ $M^{-1}$ $s^{-1}$) is known to be diffusion controlled.[36] The reverse rate coefficient ($k_{-t}$) was set to a nominally low value ($1.3 \times 10^{-5}$ $s^{-1}$), as the termination reaction is irreversible; this parameter had no effect on the simulation. Given that many of the parameters in Scheme 1 were known ($E_{Br}$, $E_S$, $k_{deact}$, $K_{Cu(II)Br}$, and $K_{Cu(I)Br}$), the only independent parameters remaining were $k_{act}$, $k_{II,d,Br}$, and $k_{I,d,Br}$, and these were refined during the simulation. For the MeCN system, where $K_{Cu(II)Br}$ was not known accurately, both $k_{II,a,Br}$ and $k_{II,d,Br}$ were allowed to refine.

Systematically varying both the concentration of EBriB and the sweep rate enabled a set of self-consistent rate coefficients to be determined (one set for MeCN and one set for DMSO) that reproduced the experimental voltammetry across the entire range of EBriB concentrations, 0−10 mM, and sweep rates, 20−1000 mV $s^{-1}$. These parameters are included in Table 1. A set of representative simulated and experimental voltammograms is shown in Figure 3 for MeCN at different concentrations of EBriB. Comparisons of a variety of other experimental and simulated voltammograms are shown in the SI. It should be reemphasized that the fits were equally good regardless of EBriB concentration, sweep rate, or solvent. A slightly lower value of $k_{act} = 7.7 \times 10^3$ $M^{-1}$ $s^{-1}$ in MeCN was reported for the $[Cu(Me_6tren)]^+$/EBriB reaction using stopped-flow methods and the radical scavenger TEMPO.[14]

In conclusion, we have developed a new technique for accurately determining the mechanistically important polymer initiator activation rate coefficient ($k_{act}$), independent of a kinetic model for the polymerization reaction. In principle, this method can be applied to any copper-catalyzed system and provides a rapid and effective way of screening prospective new copper catalysts and initiators. By varying the concentration of initiator and also altering the sweep rate, the degree of reversibility of the cyclic voltammetry $Cu^{II/I}$ wave provides a direct measure of the kinetics of the coupled activation step, and the system may be tuned so as to enable the monitoring of both rapid and slower activation reactions.

## ■ ASSOCIATED CONTENT

**Supporting Information.** Cyclic voltammetry of $[Cu(Me_6tren)]^{2+}$ in the presence and absence of bromide, spectrophotometric titrations, and comparisons of simulated and experimental voltammetry of the $[Cu(Me_6tren)]^{2+}$:EBriB system. This material is available free of charge via the Internet at http://pubs.acs.org.

## ■ AUTHOR INFORMATION

### Corresponding Author

p.bernhardt@uq.edu.au; m.monteiro@uq.edu.au

## ■ ACKNOWLEDGMENT

We gratefully acknowledge financial support from the Australian Research Council (DP0880288 to P.V.B. and FT0990978 to M.J.M.).

## REFERENCES

(1) Matyjaszewski, K.; Xia, J. *Chem. Rev.* **2001**, *101*, 2921–2990.

(2) Rosen, B. M.; Percec, V. *Chem. Rev.* **2009**, *109*, 5069–5119.

(3) Tang, H.; Arulsamy, N.; Radosz, M.; Shen, Y.; Tsarevsky, N. V.; Braunecker, W. A.; Tang, W.; Matyjaszewski, K. *J. Am. Chem. Soc.* **2006**, *128*, 16277–16285.

(4) Jakubowski, W.; Matyjaszewski, K. *Macromolecules* **2005**, *38*, 4139–4146.

(5) Jakubowski, W.; Min, K.; Matyjaszewski, K. *Macromolecules* **2005**, *39*, 39–45.

(6) Min, K.; Jakubowski, W.; Matyjaszewski, K. *Macromol. Rapid Commun.* **2006**, *27*, 594–598.

(7) Jakubowski, W.; Matyjaszewski, K. *Macromol. Symp.* **2006**, *240*, 213–223.

(8) Oh, J. K.; Tang, C.; Gao, H.; Tsarevsky, N. V.; Matyjaszewski, K. *J. Am. Chem. Soc.* **2006**, *128*, 5578–5584.

(9) Oh, J. K.; Matyjaszewski, K. *J. Polym. Sci., Part A Polym. Chem.* **2006**, *44*, 3787–3796.

(10) Oh, J. K.; Min, K.; Matyjaszewski, K. *Macromolecules* **2006**, *39*, 3161–3167.

(11) Min, K.; Jakubowski, W.; Matyjaszewski, K. *Macromol. Rapid Commun.* **2006**, *27*, 594–598.

(12) Pietrasik, J.; Dong, H. C.; Matyjaszewski, K. *Macromolecules* **2006**, *39*, 6384–6390.

(13) Magenau, A. J. D.; Strandwitz, N. C.; Gennaro, A.; Matyjaszewski, K. *Science* **2011**, *332*, 81–84.

(14) Pintauer, T.; Braunecker, W.; Collange, E.; Poli, R.; Matyjaszewski, K. *Macromolecules* **2004**, *37*, 2679–2682.

(15) Di Vaira, M.; Orioli, P. *Acta Crystallogr., Sect. B* **1968**, *24*, 595–599.

(16) Baisch, U.; Poli, R. *Polyhedron* **2008**, *27*, 2175–2185.

(17) Barbucci, R.; Campbell, M. J. M. *Inorg. Chim. Acta* **1975**, *15*, L15–L16.

(18) Barbucci, R.; Bencini, A.; Gatteschi, D. *Inorg. Chem.* **1977**, *16*, 2117–2120.

(19) Barbucci, R.; Mastroianni, A.; Campbell, M. J. M. *Inorg. Chim. Acta* **1978**, *27*, 109–114.

(20) Ehsan, M. Q.; Ohba, Y.; Yamauchi, S.; Iwaizumi, M. *Bull. Chem. Soc. Jpn.* **1996**, *69*, 2201–2209.

(21) Hempel, J. C.; Miller, M. E. *J. Chem. Phys.* **1981**, *75*, 2959–2970.

(22) Deeth, R. J.; Gerloch, M. *Inorg. Chem.* **1985**, *24*, 4490–4493.

(23) Becker, M.; Heinemann, F. W.; Schindler, S. *Chem.—Eur. J.* **1999**, *5*, 3124–3129.

(24) Bortolamei, N.; Isse, A. A.; Di Marco, V. B.; Gennaro, A.; Matyjaszewski, K. *Macromolecules* **2010**, *43*, 9257–9267.

(25) Pintauer, T.; Reinoehl, U.; Feth, M.; Bertagnolli, H.; Matyjaszewski, K. *Eur. J. Inorg. Chem.* **2003**, 2082–2094.

(26) Clark, W. M. *The Oxidation—Reduction Potentials of Organic Systems*; The Williams and Wilkins Co.: Baltimore, MD, 1960.

(27) Braunecker, W. A.; Tsarevsky, N. V.; Gennaro, A.; Matyjaszewski, K. *Macromolecules* **2009**, *42*, 6348–6360.

(28) Binstead, R. A. *SPECFIT*, global analysis system; Spectrum Software Associates: Marlborough, MA, 2007.

(29) De Paoli, P.; Isse, A. A.; Bortolamei, N.; Gennaro, A. *Chem. Commun.* **2011**, *47*, 3580–3582.

(30) Lincoln, S. F.; Coates, J. H.; Doddridge, B. G.; Hounslow, A. M.; Pisaniello, D. L. *Inorg. Chem.* **1983**, *22*, 2869–2872.

(31) Bard, A. J.; Faulkner, L. R. *Electrochemical Methods: Fundamentals and Applications*, 2nd ed.; Wiley: New York, 2001.

(32) Rudolf, M.; Feldberg, S. W. *DigiSim*, version 3.03b; Bioanalytical Systems Inc.: West Lafayette, IN, 2004.

(33) Monteiro, M. J.; Guliashvili, T.; Percec, V. *J. Polym. Sci., Part A Polym. Chem.* **2007**, *45*, 1835–1847.

(34) Matyjaszewski, K.; Paik, H. J.; Zhou, P.; Diamanti, S. J. *Macromolecules* **2001**, *34*, 5125–5131.

(35) Tang, W.; Kwak, Y.; Braunecker, W.; Tsarevsky, N. V.; Coote, M. L.; Matyjaszewski, K. *J. Am. Chem. Soc.* **2008**, *130*, 10702–10713.

(36) Johnston-Hall, G.; Monteiro, M. J. *J. Polym. Sci., Part A Polym. Chem.* **2008**, *46*, 3155–3173.